Supporting information for:

The Role of Central Gold Atom in Ligand-Protected Biicosahedral Au_{24} and Au_{25} Clusters

Jing-Qiang Goh,[†,‡] Sami Malola,[¶] Hannu Häkkinen,[¶] and Jaakko Akola[*,†,‡]

Department of Physics, Tampere University of Technology, P.O. Box 692, FI-33101 Tampere, Finland, COMP Centre of Excellence, Department of Applied Physics, Aalto University, FI-00076 Aalto, Finland, and Departments of Physics and Chemistry, Nanoscience Center, University of Jyväskylä, FI-40014 Jyväskylä, Finland

E-mail: jaakko.akola@tut.fi

[*]To whom correspondence should be addressed
[†]Tampere University of Technology
[‡]Aalto University
[¶]University of Jyväskylä

Computational Methods - CP2K, CPMD, GPAW

The preliminary geometry optimization of all clusters and the vibrational analysis of the clusters **3** and **3'** have been performed using the CP2K program package.[S1,S2] This method uses two representations of the electron density: localized Gaussian and plane wave (GPW) basis sets. The Gaussian functions are used for the Kohn-Sham orbitals while the plane waves describe electron density only enabling more efficient treatment of molecular systems than traditional plane wave codes. The valence electron-ion interaction is based on the norm-conserving and separable pseudopotentials of the analytical form derived by Goedecker, Teter, and Hutter (GTH).[S3] We considered the $5d^{10}6s^1$ valence configuration for Au, and the optimized pseudopotential includes scalar relativistic corrections via an averaged potential. For the Gaussian-based (localized) expansion of the Kohn-Sham orbitals we used a library of contracted m-DZVP basis sets,[S4] and the complementary plane wave basis set has a cut-off of 400 Ry for electron density. The generalized gradient-corrected approximation of Perdew, Burke, and Ernzerhof (PBE) is adopted for the exchange-correlation energy functional.[S5]

The structural parameters and effective charges of clusters **2/2'** are displayed in Tables S1 and S2. See also Figure S1 for the visualization of charges. On average, the Au−Au distances are 4.1% larger than in the experiments (compare 2.5-2.7% for CPMD with the same functional), and the interplanar *b*-*c* distance is 0.22 Å larger. Part of this deviation can be ascribed to the m-DZVP basis set in CP2K, and we decided to re-optimize the structures with the CPMD method for a more accurate description of structural parameters in the main text.

For the CPMD calculations, we use the TPSS exchange-correlation functional in addition to PBE in order to obtain an improved structural description of the nanoclusters in comparison with the experimental results. The CPMD simulations employ the norm-conserving and scalar-relativistic pseudopotentials by Troullier and Martins (Ref.[S6]). The valence configurations and local components are: Au, $5d^{10}6s^1$ (*s* local, cutoff 2.20 a_0); S, $3s^23p^4$ (*p* local, 1.45 a_0); P, $3s^23p^3$ (*p* local, 1.50 a_0); Cl, $3s^23p^5$ (*p* local, 1.45 a_0); C, $2s^22p^2$ (*p* local, 1.23 a_0); and H, $1s^1$ (*s* local, 0.50 a_0). In addition to valence states, we have included the nonlocal 6p- and 5f-channels (cutoff

2.60 a_0 and 1.60 a_0, respectively) for the Au pseudopotential based on an excited atomic configuration $5d^9 6s^{0.8} 6p^{0.1} 5f^{0.1}$, where it is important to avoid so-called "ghost states" referring to unbound orbitals by removing charge from lower lying orbitals (here: 5d-shell). We also used the nonlinear core corrections for the Au pseudopotential with a cutoff distance 1.90 a_0 for the core charge.[S7]

The GPAW method is used for the analysis of superatomic electronic states (projection of the Kohn-Sham wavefunctions to the spherical harmonics), and for the calculations of the optical absorption and circular dichroism spectra, because GPAW contains the necessary options and tools for these purposes. Here, we first optimized the structures using the local density approximation (LDA) exchange-correlation functional to obtain better structural agreement with the reported experimental structures (in particular shorter Au−Au bond distances), as the optical spectra are sensitive to this detail. The following GPAW calculations are performed with the PBE exchange-correlation functional for fixed geometries.

Table S1: Structural parameters of the clusters 2 and 2', respectively. Labels as in Table 1 of main text. Note that the experimental structural result is not available for the cluster 2. The geometry optimizations were performed with the CP2K program using the PBE functional.

	Cluster **2**	Cluster **2'**	
	PBE	PBE	Exp. Ref[S8]
	Distances (Å)		
Au–Au	2.962 (0.107)	2.985 (0.105)	2.868 (0.084)
Au^b–Au^c	3.074 (0.046)	3.232 (0.062)	3.015 (0.059)
Au_C–Au	—	2.994 (0.025)	2.87 (0.030)
Au_I–Au	2.834 (0.014)	2.865 (0.052)	2.759 (0.038)
Au–P	2.364 (0.005)	2.372 (0.004)	2.311 (0.024)
Au–S	2.435 (0.008)	2.432 (0.080)	2.388 (0.024)
S–C	1.854 (0.004)	1.854 (0.005)	1.824 (0.102)
	Angles (deg)		
Au–S–Au	78.3 (1.8)	83.2 (2.3)	78.3 (2.1)
Au–S–C	105.0 (1.2)	105.0 (1.2)	103.5 (2.5)
Au–P–C	114.3 (1.6)	114.0 (1.6)	112.4 (2.9)
S–C–C	110.7 (0.6)	111.0 (0.6)	108.8 (5.9)

Table S2: Average Bader charges of the clusters 2 and 2'. Labels as in Table S1 and Au_V refers to the vertex Au atoms. The total charges of the Au core and different groups are reported in the lower part.

Atom	**2**	**2'**
Au_C	—	0.03
Au_I	-0.21	-0.20
Au_V	0.02	0.09
$Au^{a,d}$	-0.03	-0.03
$Au^{b,c}$	0.03	0.04
S	-0.21 (0.06)	-0.18
P	-0.03 (0.10)	-0.02
Cl	-0.60 (0.00)	-0.57
Au_{24} / Au_{25} (total)	-0.38	-0.07
$(Ph_3)_{10}$	3.48	3.98
$(SC_2H_5)_5$	-0.88	-0.76
Cl_2	-1.21	-1.15

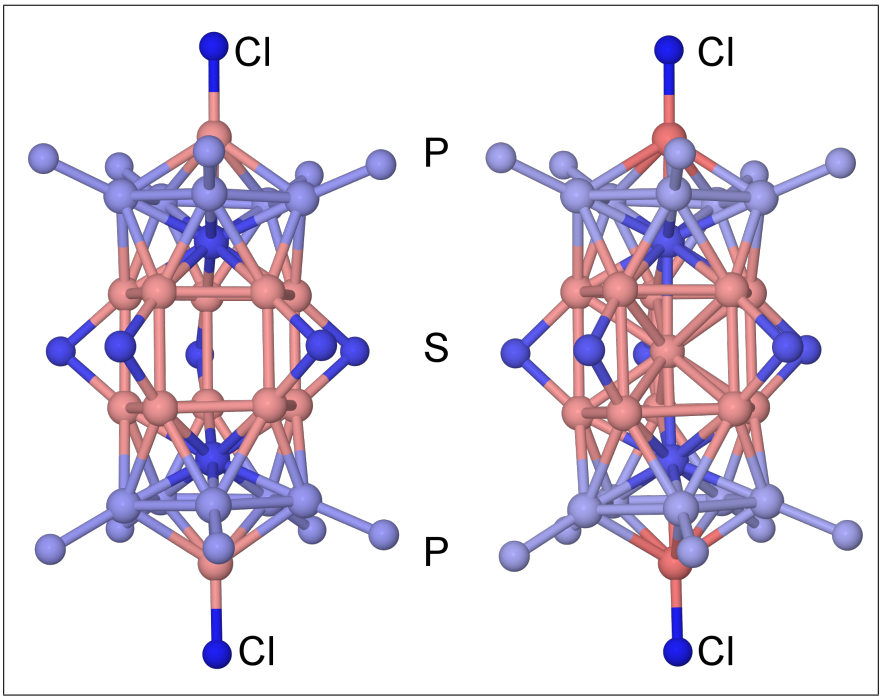

Figure S1: Visualization of Bader charge distribution for the clusters **2** and **2'** (aromatic and alkane side groups are omitted). The color scale ranges from red (positive charge) to blue (negative charge).

Table S3: Table of relative contributions of different states to total intensity of the 1st feature around 620 nm in the absorption spectrum of the cluster 1 (Au_{24}). Contribution percentage of transitions from/to specific occupied (Occ.) and unoccupied (Unocc.) Kohn-Sham states around Fermi energy are listed separately with the center of mass (COM) symmetry (projection with respect to Au_C) assignments shown in the Fig 3 of main text.

Occ.	COM symmetry	Contribution (%)	Unocc.	COM symmetry	Contribution %
HOMO	S	1.60	LUMO	D	1.87
HOMO-1	P	86.86	LUMO+1	D	1.62
HOMO-2	D	1.32	LUMO+2	S	87.16
HOMO-3	D	1.76	LUMO+3	F	0.17
HOMO-4	F	0.86	LUMO+4	F	0.20
rest		7.60	rest		8.98
Total		100.00	Total		100.00

Table S4: Table of relative contributions of different states to total intensity of the 1st feature around 680 nm in the absorption spectrum of the cluster 1' (Au_{25}). Contribution percentage of transitions from/to specific occupied (Occ.) and unoccupied (Unocc.) Kohn-Sham states around Fermi energy are listed separately with the center of mass (COM) symmetry (projection with respect to Au_C) assignments shown in the Fig 3 of main text.

Occ.	COM symmetry	Contribution (%)	Unocc.	COM symmetry	Contribution %
HOMO	S	0.27	LUMO	S	93.65
HOMO-1	D	1.36	LUMO+1	D	0.67
HOMO-2	D	1.44	LUMO+2	D	0.59
HOMO-3	P	66.57	LUMO+3	F	0.09
HOMO-4	F	3.93	LUMO+4	F	0.07
rest		26.43	rest		4.93
Total		100.00	Total		100.00

References

(S1) CP2K Developers Group. `http://www.cp2k.org`, 2000-2013.

(S2) VandeVondele, J.; Krack, M.; Mohamed, F.; Parrinello, M.; Chassaing, T.; Hutter, J. Quickstep: Fast and Accurate Density Functional Calculations Using a Mixed Gaussian and Plane Waves Approach. *Comput. Phys. Commun.* **2005**, *167*, 103–128.

(S3) Goedecker, S.; Teter, M.; Hutter, J. Separable Dual-Space Gaussian Pseudopotentials. *Phys. Rev. B* **1996**, *54*, 1703–1710.

(S4) VandeVondele, J.; Hutter, J. Gaussian Basis Sets for Accurate Calculations on Molecular Systems in Gas and Condensed Phases. *J. Chem. Phys.* **2007**, *127*, 114105–1–9.

(S5) Perdew, J. P.; Burke, K.; Ernzerhof, M. Generalized Gradient Approximation Made Simple. *Phys. Rev. Lett.* **1996**, *77*, 3865–3868.

(S6) Troullier, N.; Martins, J. L. Efficient Pseudopotentials for Plane-Wave Calculations. *Phys. Rev. B* **1991**, *43*, 1993–2006.

(S7) Louie, S. G.; Froyen, S.; Cohen, M. L. Nonlinear Ionic Pseudopotentials in Spin-Density-Functional Calculations. *Phys. Rev. B* **1982**, *26*, 1738–1742.

(S8) Shichibu, Y.; Negishi, Y.; Watanabe, T.; Chaki, N.; Kawaguchi, H.; Tsukuda, T. Biicosahedral Gold Clusters $[Au_{25}(PPh_3)_{10}(SC_nH_{2n+1})_5Cl_2]^{2+}$ (n=2-18): A Stepping Stone to Cluster-Assembled Materials. *J. Phys. Chem. C* **2007**, *111*, 7845–7847.